Arch. Metall. Mater. **63** (2018), 4, 1735-1741

DOI: 10.24425/amm.2018.125099

R. KAWULOK*#, P. KAWULOK*, I. SCHINDLER*, P. OPĚLA*, S. RUSZ*, V. ŠEVČÁK*, Z.SOLOWSKI**

STUDY OF THE EFFECT OF DEFORMATION ON TRANSFORMATION DIAGRAMS OF TWO LOW-ALLOY MANGANESE-CHROMIUM STEELS

The work deal with an assembling and comparing of transformation diagrams of two low-alloy steels, specifically 16MnCrS5 and 20MnCrS5. In this work, diagrams of the type of CCT and DCCT of both steels were assembled. Transformation diagrams were assembled on the basis of dilatometric tests realized on the plastometer Gleeble 3800, of metallographic analyses and of hardness measurements. In addition, for comparison, the transformation diagrams were assembled even with use of the QTSteel 3.2 software. Uniform austenitization temperature of 850°C was chosen in case of both steels and even both types of diagrams. In case of both steels, an influence of deformation led to expected acceleration of phase transformations controlled by diffusion and also of bainite transformation. In both cases, the kinetics of martensitic transformation was not significantly affected by deformation.

Keywords: CCT and DCCT diagrams, 16MnCrS5 and 20MnCrS5 steels, Dilatometric tests, Microstructure

1. Introduction

Knowledge of transformation kinetics of selected steels is necessary for the achievement of the required structure and, thus, required mechanical properties [1,2]. Suitable tools for the description of the kinetics of transformations under conditions of changing temperature in time are transformation diagrams of CCT type (Continuous Cooling Transformation). For the cases of controlled forming and cooling, larger usability has diagrams of DCCT type (Deformation Continuous Cooling Transformation), which – compared to classical diagrams – also include influence of the prior deformation, which has indispensable effect to the kinetics of steel transformations [3,4]. Of course, the transformation products emerging during cooling are mostly dependent on the chemical composition. Also, they are affected by factors such as a cooling rate, austenitization conditions, previous deformation, strain rate and austenitic grain size [5,6]. A general view to the effect of these parameters to the CCT diagram is shown in Fig. 1 [7].

All alloying elements, excepting Si, Co and Al, increase stability of austenite, and therefore displace the curves of the beginning and end of the diffusion transformations (ferrite and pearlite) to the right. A study of issues of deformation influence on bainite transformation reveals that all alloying elements excepting Co decrease temperature of the beginning of the bainite transformations, and that is especially C, Cr, Mo, Ni, Mn, W. Also, in case of martensitic transformation, this transformation, respectively temperature of the beginning of this transformation is decreased by all elements dissolved in austenite with the exception of aluminum and cobalt [8-13].

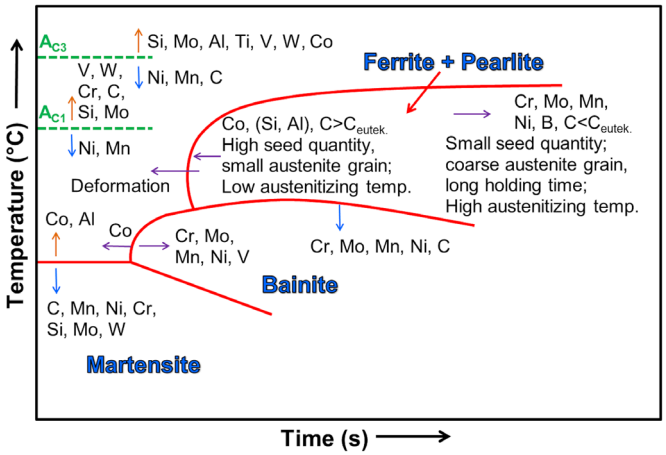

Fig. 1. Effect of alloying, thermomechanical factors and structure state on transformation kinetics [7]

Transformation of plastically deformed austenite to ferrite or pearlite proceeds at higher temperatures than in austenite without a previous deformation, which also affirms by series of works. According to the team of authors [14], the effect of acceleration is expressed mainly at the beginning of these transformations and increases with a growing deformation. The results of the effect of plastic deformation to the bainite transformation differ dependent on the value of strain and especially on a chemi-

* VSB-TECHNICAL UNIVERSITY OF OSTRAVA, FACULTY OF METALLURGY AND MATERIALS ENGINEERING, 17. LISTOPADU 15/2172, 708 33 OSTRAVA – PORUBA, CZECH REPUBLIC
** TŘINECKÉ ŽELEZÁRNY, A.S., PRŮMYSLOVÁ 1000, 739 61 TŘINEC, CZECH REPUBLIC
# Corresponding author: rostislav.kawulok@vsb.cz

cal composition of steel. An effect of the plastic deformation to the austenite transformation to martensite has mostly a slightly deceleration effect. During deformation of austenite, a dense dislocation network is generated, which brakes proceeding of the phase boundary and in spite of a big number of nucleuses, a share of a new phase is sometimes lower. However, an opposite phenomenon sometimes happens, when accumulated latticed defects initiate creation of martensite, and it then starts creation at higher temperatures than in case of transformation of non-deformed austenite [1,6,15-17].

Ferrite and pearlite transformation is also highly dependent on the austenitic grain size, since this transformation proceeds with help of a diffusion mechanism which also uses sequential growth for nucleation, first of all, of boundaries of grains. So, it is clear that the finer austenitic grain is, the more grain boundaries are in the matrix, and therefore more nucleus places, which will cause a growth of temperature of ferrite and pearlite origination, and, thus, acceleration of the both transformations. A higher austenitic grain supports a martensitic transformation by increasing temperature of its beginning M_s. It means that the higher austenitization temperature is, the longer dwell time is at this temperature, and thus the more austenitization grain grows and, as a result, temperature M_s grows [1,6,18].

However, a cooling rate essentially effects the structure and therefore to mechanical properties. Very different cooling rates then can affect both kinetics and kind of phase transformations, when with growing rate, the probability of hardening structures, such as bainite and martensite, grows as well [5,15,19].

The aim of this work was to assess influence of chemical composition, especially a combination of content of C, Mn and Cr, in combination with a previous deformation to the transformation kinetics of two adjacent steels. Concretely, it was steels 16MnCrS5 and 20MnCrS5 that belong to category of low-carbon hypoeutectoid steels with the use for semi-loaded parts of machines and vehicles. Chemical composition of the both steels is specified in Table 1 [20]. These steels were chosen because of their almost identical chemical composition which slightly differs mainly in the content of mentioned elements (C, Mn and Cr). In addition, the both steels were delivered in the same structure state – in the form of rods with the diameter of 20 mm, hot rolled by the same deformation level.

TABLE 1

Chemical composition of selected steels in wt. % [20]

Steel grade	C	Mn	Cr	Si	S	P
16MnCrS5	0.14-0.19	1.00-1.30	0.80-1.10	max. 0.40	max. 0.035	max. 0.035
20MnCrS5	0.17-0.22	1.10-1.40	1.00-1.30	max. 0.40	max. 0.035	max. 0.035

2. Experiment description

For assessment of the effect of carbon and chromium and a prior deformation to kinetics of transformation of the assessed steels, there were used dilatometric analyses which were performed on a contact dilatometric module of the plastometer Gleeble 3800. The plastometer Gleeble 3800 in combination with a dilatometric module allows application of compressive or tensile deformations, which is not standard for all dilatometers [21-23].

Two types of specimens were prepared for dilatometric tests. For dilatometric tests without deformation, there were produced specimens with a diameter of 10 mm and total length of 84 mm with hollow head parts and a reduced central part of the specimen with a diameter of 5 mm and length of 5 mm. This type of specimens is not suitable for the application of compressive deformations, and therefore for dilatometric tests with effect of deformations, cylindrical specimens of SICO type with a diameter of 10 mm and the heated part length of 20 mm were selected. Unfortunately, disadvantage of these specimens is the maximum cooling rate which achieves up to 50°C/s. This limit often does not allow us to describe the entire area of transformations in a (D)CCT diagram, because in some cases of especially low-carbon steels, selected transformations proceed even at higher cooling rates [5,21].

All dilatometric tests (without deformation and with deformation for the both steels) were realized after unified austenitization at temperature of 850°C and dwell of 180 s. Specimens determined for the dilatometric tests without deformation were consequently cooled with constant rates up to the room temperature. For a complete description of the CCT diagram of the steel 20MnCrS5, the range of cooling rate was 0.16-20°C/s, while for the steel 16MnCrS5 the range of rate was relatively wider: 0.16-100°C/s.

In case of dilatometric tests with an effect of a prior low-temperature deformation, the specimens after heating-up and dwelling at temperature of 850°C were deformed with a uniaxial compression by a true strain of 0.35 and strain rate of 1 s^{-1} and consequently cooled with selected rates to temperature of 25°C. For an objective description of the DCCT diagram of the steel 20MnCrS5, the maximum rate of 35°C/s was suitable, while for the steel 16MnCrS5, as was expected, the resulting DCCT diagram was not fully complete even after cooling with a rate

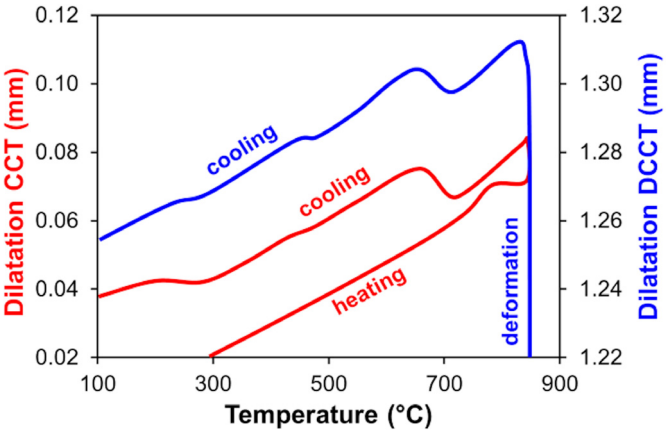

Fig. 2. Example of influence of prior deformation upon shape of dilatation curves (cooling with rate of 5°C/s) of the steel 16MnCrS5

of 50°C/s. For assessment of the obtained dilatation curves, specialized CCT software was used supplied by DSI Company together with the plastometer Gleeble. An example of deformations of non-affected and affected dilatation curves of the steel 16MnCrS5 after cooling with a rate of 5°C/s is shown in Fig. 2. Selected dilatometrically tested specimens were consequently subjected to metallographic analyses and measurements of hardness HV30.

For comparing, the both steels were subjected – for the same conditions as in the physical experiment – to a numeric design of the both types of diagrams, which is possible thanks to QTSteel 3.2 Software [24].

3. Results and discussion

Based on confrontation of the dilatation curves analysis and metallographic analyses, final transformation diagrams were compiled. An example of such diagram is the DCCT Diagram of the steel 20MnCrS5 – Fig. 3.

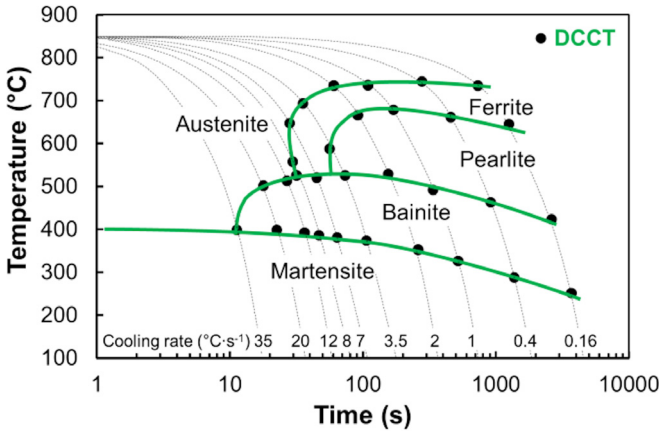

Fig. 3. Example of designing DCCT transformation diagram of the steel 20MnCrS5

To assess the effect of the chemical composition, common CCT (see Fig. 4) and DCCT (see Fig. 5) diagrams, which clearly documents an effect of the chemical composition, were designed. The cooling rates curves are integrated into the diagrams just for visualization because they were not uniform for both steels. Based on the both types of the comparing transformation diagrams (CCT and DCCT), it is clear seen an effect of a slightly increased share of the combination of C, Mn and Cr (Δwt. % (C + Mn + Cr) = 0.05 wt. %), which led to displacement of all transformations in the right direction to slower cooling rates, whereby there were precisely verified assumptions about deceleration of all types of transformations in general by all elements with the exception of Si, Co and Al [7-9]. In particular from the point of view of the kinetics of the ferrite and pearlite transformation, there was verified that these transformations are significantly affected first of all by Mn and C, whereas both these transformations decelerate. To be more precisely, the both above-mentioned elements decelerate diffusion and by this decrease temperature of the beginning of this transformation as well as displace the entire area of ferrite in the CCT diagrams to the right [7,10].

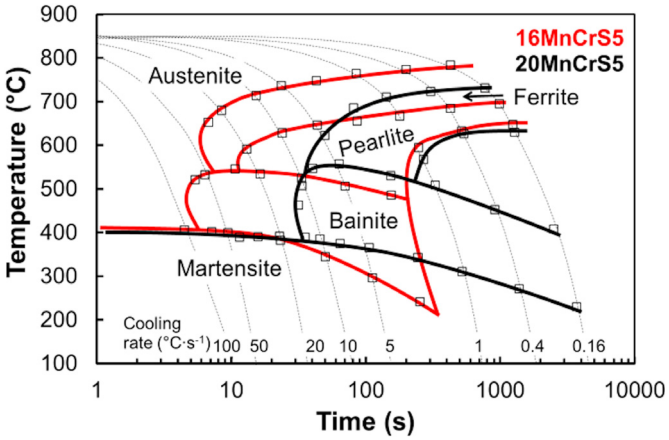

Fig. 4. Combination of CCT diagrams of the steel 16MnCrS5 and 20MnCrS5

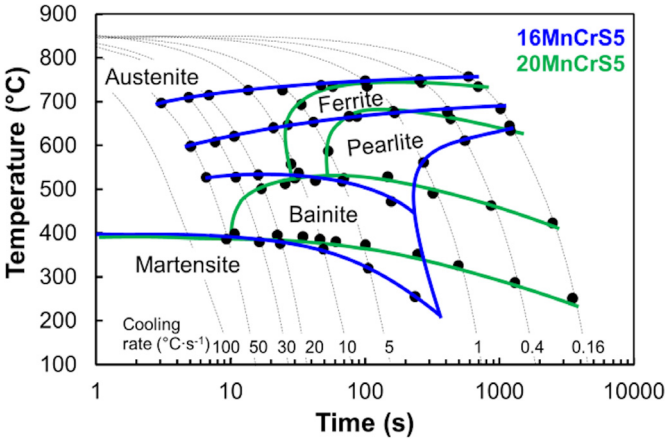

Fig. 5. Combination of DCCT diagrams of the steel 16MnCrS5 and 20MnCrS5

Again, for easier analysis of the deformation effect, the CCT and DCCT diagrams were merged in comparing diagrams, and that is for the both steel represented in Figs. 6,7.

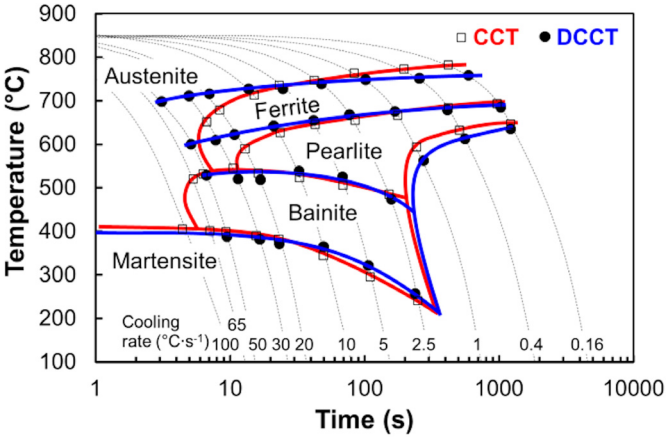

Fig. 6. Combination of CCT and DCCT diagram of the steel 16MnCrS5

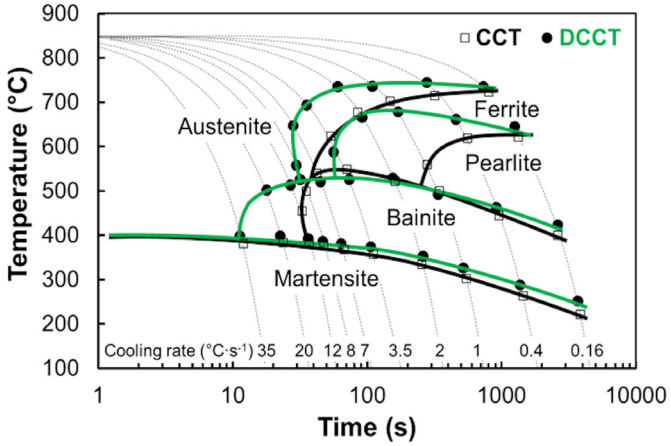

Fig. 7. Combination of CCT and DCCT diagram of the steel 20MnCrS5

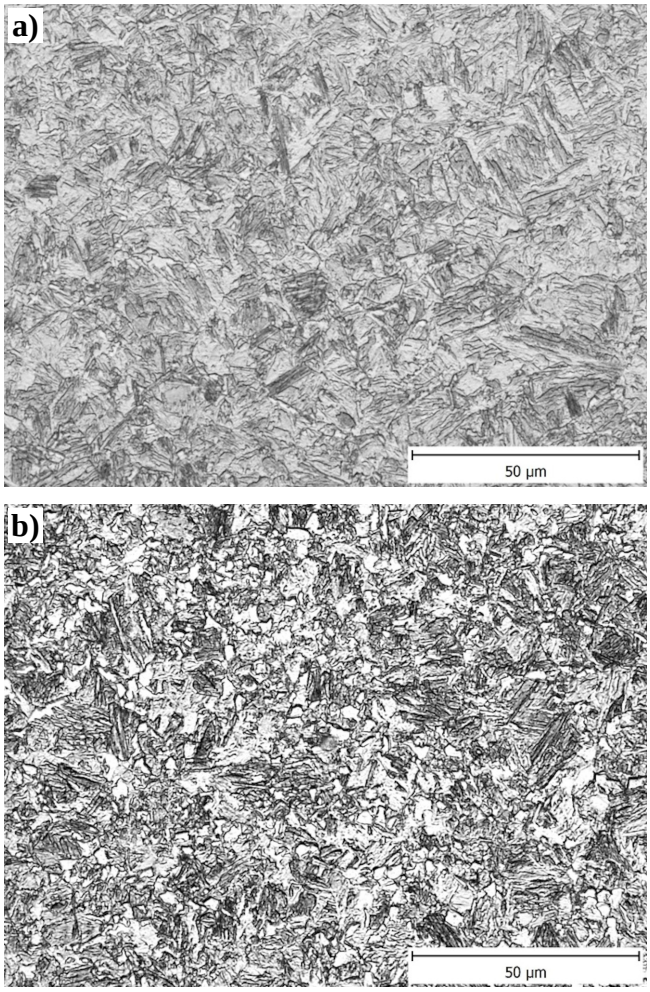

Fig. 8. a) Without deformation – cooling rate of 50°C·s^{-1} – 75% Martensite + 25% Bainite-, b) After deformation – cooling rate of 50°C·s^{-1} – 20% Ferrite + 14% Pearlite + 36% Bainite + 30% Martensite Comparison of microstructure and shares of phases of the steel 16MnCrS5 without and after deformation of selected rates

First of all, by visual checking the comparing diagram of the steel 20MnCrS5 in Fig. 7, it is clear that transformations controlled by a diffusion mechanism – Ferrite and Pearlite – were accelerated. In case of the steel 16MnCrS5 (see Fig. 6), it is not entirely clear at first glance, nevertheless for the limit cooling rate of 50°C/s, these components (Ferrite and Pearlite) in the CCT diagram were not already detected, while in the DCCT diagram – yes. On the basis of this information, it is possible thus assume that in both cases there was verified a thesis that quantity of lattice defects is increased due to deformation, which supports diffusion of all atoms in solid solution and leads to a quicker nucleation and growth of nucleuses of a new phase [1,6]. It was also similar in case of a bainite transformation which was again more expressively accelerated in case of the steel 20MnCrS5; however even in case of the steel 16MnCrS5 it can be expected because it is proved by microstructural analyses and development of the structural shares. Deformation had almost negligible effect to the values of temperature of the beginning of the martensitic transformation, and that is in both steels.

The method of classic light microscopy was used to analyze and evaluate the microstructure. This method in combination with the evaluating software QuickPHOTO INDUSTRIAL provided necessary information about presence of individual structural components and, at the same time, their shares in the structure. This software is working on the basis of structure differentiation by means of the own database, when the shares of individual components are evaluated on the basis of their color spectrum. In Fig. 8. there are purposely presented images of the microstructure of the steel 16MnCrS5 without influence of the previous deformation after cooling with a rate of 50°C/s, which is entirely bainite-martensitic, and with influence of the previous deformation, which consists of a complete quaternion of the structural components. In Fig. 9, for comparison, there are specimens microstructures of the steel 20MnCrS5 – unaffected and affected by the previous deformation and after the cooling by the rate of 2°C/s. In case of the specimen – unaffected by previous deformation – the structure is partly formed by polyhedral ferrite supplemented about of quenching phases – bainite and martensite. In case of by-deformation-effected structure (Fig. 9b) an accelerating effect of pearlite transformation was confirmed. This occurred because the structure was at the cooling rate of 2°C/s formed by complete quaternion of structural components – including pearlite which was not detected in the no-deformed structure (Fig. 9a).

Developments of the structural components for the both variants of the diagrams and both steels are shown in Fig. 10. These graphical dependences of the shares of separate components and hardness on the cooling rate are useful mainly for clarification of changes of hardness, which of cause is dependent just on the structural composition. The hardness was measured by three indentations – the results of individual indentations were in case of specific specimen (cooling rate) averaged, when the deviation of hardness measurement of the individual indentations was always below of 5%. This procedure has confirmed the structure homogeneity and thus even hardness values itself – so, the data could not be affected for instance by the hardness measurement near the specimen rim. In case of the steel 16MnCrS5, it is also clear that the previous deformation really significantly accelerated a bainite transformation, because by comparing

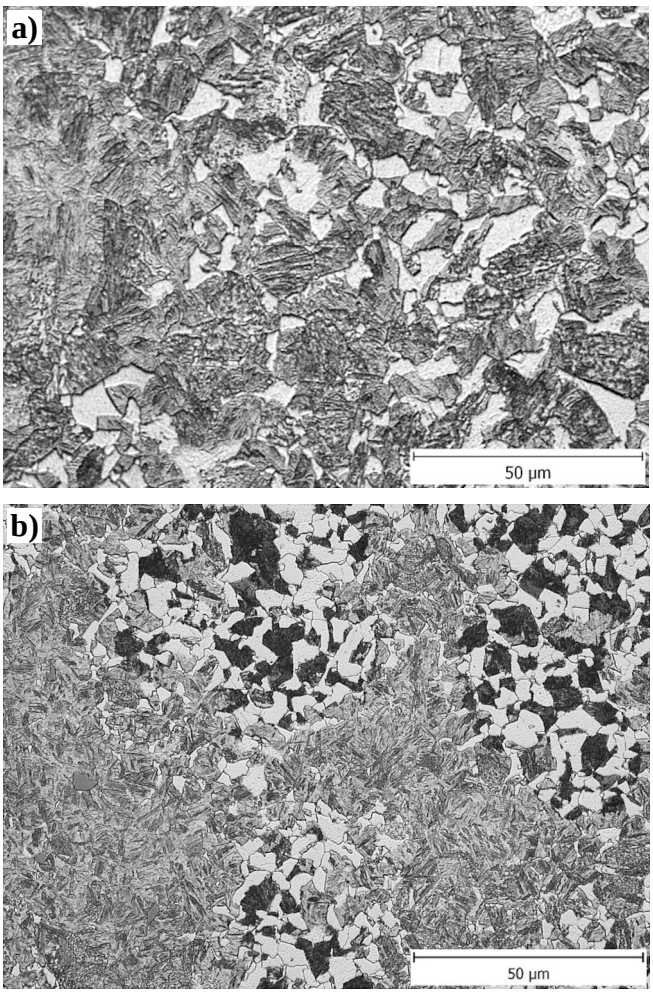

Fig. 9. a) Without deformation – cooling rate of 2°C·s^{-1} – 15% Ferrite + 39% Martensite + 46% Bainite-, b) After deformation – cooling rate of 2°C·s^{-1} – 20% Ferrite + 5% Pearlite + 40% Bainite + 35% Martensite Comparison of microstructure and shares of phases of the steel 20MnCrS5 without and after deformation of selected rates

the structural composition it is clear that the structures of the deformed specimens, which were cooled with rates higher than 20°C/s were mostly consisted of bainite (see Fig. 10b). While martensite predominated in the structures of the specimens non-deformed and cooled with the same rate (see Fig. 10a). It was not the same in the steel 20MnCrS5. In this case, deformation affected structural shares just up to the level where it doesn't affect the order of the presented components.

For comparison and verification of the usability of the numeric simulation in cases of a compiling of the transformation diagrams, these diagrams were also compiled with the use of a specialized QTSteel 3.2 Software. With help of specialized software programs, the compiling of the transformation diagrams is significantly simpler than in case of physical testing, but satisfied results are not always reached [3,22,24]. Transformation diagrams for both versions (CCT and DCCT) of both assessed steels simulated in the QTSteel are shown in Fig. 11. By comparing diagrams from the QTSteel (see Fig. 11) with diagrams compiled on the basis of dilatometry (see Figs. 6,7), it is possible to claim that generally better agreements were achieved in CCT

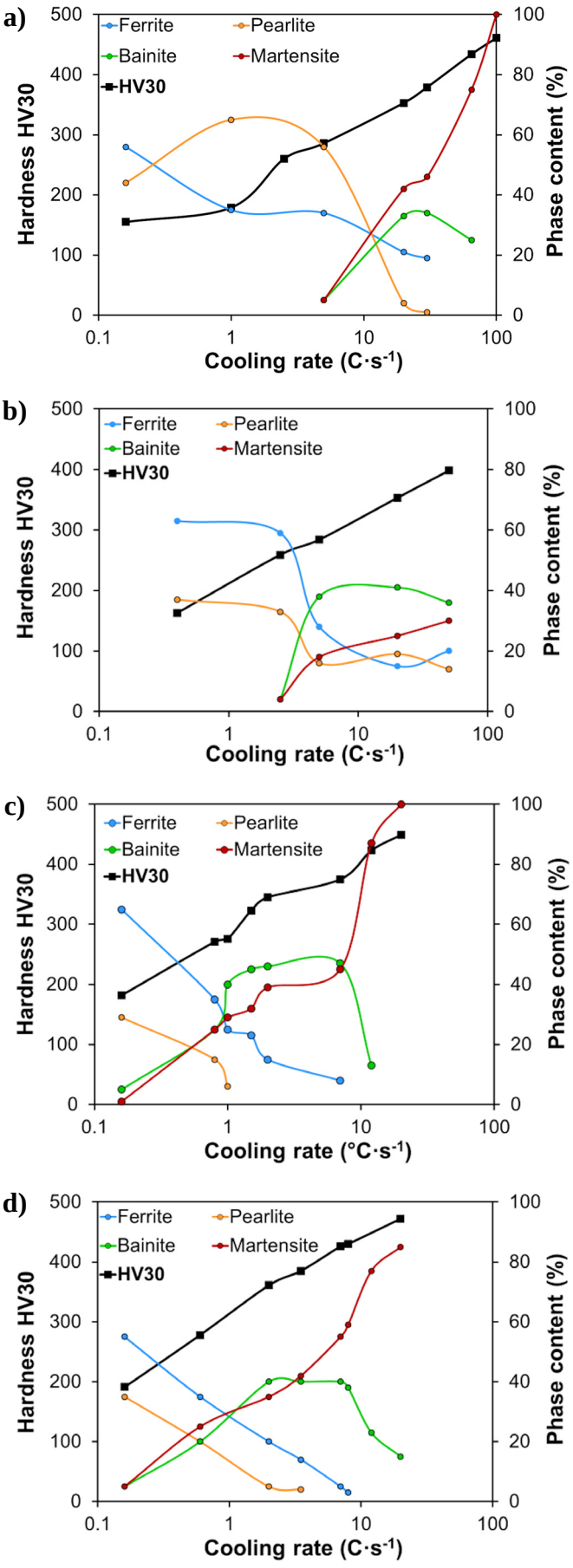

Fig. 10. a) CCT – 16MnCrS5-, b) DCCT – 16MnCrS5-, c) CCT – 20MnCrS5-, d) DCCT – 20MnCrS5 Development of structural shares and measured hardness of HV30 depending on cooling rate

version, nevertheless there are slight inaccuracies. Unfortunately, in case of diagrams affected by previous deformations (DCCT), mainly in the steel 16MnCrS5, this modeling is totally insufficient, because none of these types of transformations corresponds to the experimental reality. In particular from the point of view of temperatures, transformations of austenite to ferrite, pearlite and bainite are displaced to higher temperatures in the QTSteel. In addition, the decrease of temperature of the beginning of the martensitic transformation at the decreasing cooling rate is not respected in all cases of the numerically modelled diagrams.

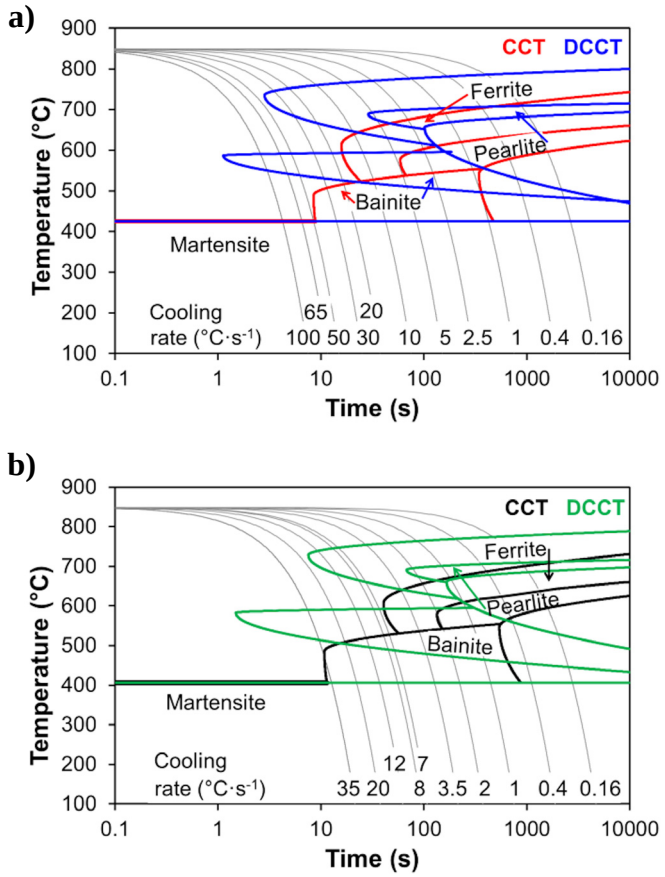

Fig. 11. a) 16MnCrS5, b) 20MnCrS5, CCT and DCCT diagrams of the steels 16MnCrS5 and 20MnCrS5 designed with help of the QTSteel 3.2. Software

Differences between the dilatometrically designed diagrams and diagrams calculated in the QTSteel software are additionally demonstrated by means of graphical illustration of the development of the HV30 hardness values in Fig. 12. As is clear here, of caurse, hardness in the both cases grows with the increasing cooling rate. Nevertheless, in case of the QTSteel Software, the development of hardness is dramatically affected by structural shares but compared with the experiment it is clear that this is really true only in some cases. In case of experiments, it was rather a gradual growth in all variants. Based on a graphical dependence of HV30 hardness after mathematic modeling in the QTSteel, there is evident an algorithm, which due to deformation displaces structural shares and thus also hardness towards higher cooling rates.

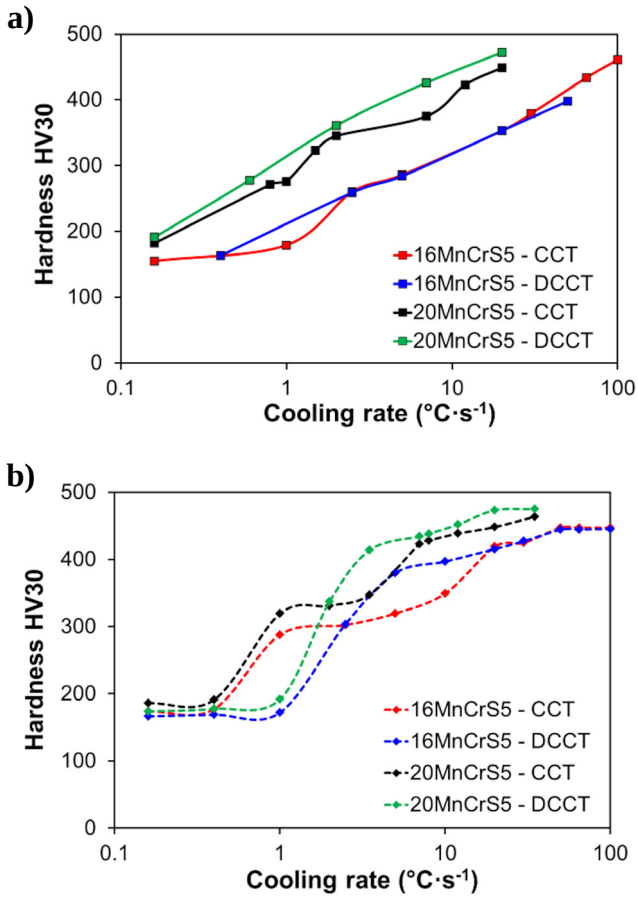

Fig. 12. a) Dilatometric tests-, b) Software QTSteel 3.2 Comparing the effect of deformation and cooling rate on hardness

4. Conclusions

Based on dilatometric tests in combination with metallographic analyses and measurements of hardness, CCT and DCCT transformation diagrams of the steel 16MnCrS5 and 20MnCrS5 were designed. Since all diagrams were designed on the basis of unified conditions of austenitization (850°C – 3 minutes), they could well serve for the assessment of the effect of chemical composition and deformation on the kinetics of transformations of low-alloyed hypoeutectoid steels.

From the point of view of influence of chemical composition, there was verified an assumption of influence of carbon, chromium and manganese which in steel 20MnCrS5 were in general slightly higher. A slightly increased content of these elements caused a displacement of the area of ferrite, pearlite, bainite and martensite to the right towards longer times and lower cooling rates, and that is for the both variants of the diagrams (CCT and DCCT).

In case of analysis of influence of a prior deformation to the kinetics of transformations in the both assessed hypoeutectoid steels there was also confirmed an assumption of acceleration of ferrite and pearlite transformation, so transformations which are controlled by diffusion. Beside of that, considerable acceleration of the bainite transformation due to the prior deformation was proved. Thus, there was sustained a thesis that a creation of

nucleuses of a new phase is accelerated in a deformed austenite at a bainite transformation, because they are firstly created in deformed bands as narrow ferrite particles which are rimmed by carbides [25,26]. In case of influencing the martensitic transformation, no fundamental effect of the prior deformation was evident.

Further this work took into consideration a possibility of using of numeric simulation for designing the transformation diagrams of CCT and DCCT types. Concretely, it was about usability of the QTSteel 3.2 Software. Based on the obtained results, it is possible to recommend this software for designing diagrams non-affected by deformations (CCT), however in case of DCCT diagrams, this software is too far from the experimental reality. So, for this complicated problem, experimental methods continue to be more suitable, for example, dilatometry supported by metallographic analyses.

Acknowledgements

This paper was created at the Faculty of Metallurgy and Materials Engineering within the Project No. LO1203 "Regional Materials Science and Technology Centre - Feasibility Program" funded by the Ministry of Education, Youth and Sports of the Czech Republic; and within the students' grant project SP2018/105 supported at the VŠB – TU Ostrava by the Ministry of Education of the Czech Republic.

REFERENCES

[1] F. Nürnberger, O. Grydin, M. Schaper, F.W. Bach, B. Koczurkiewicz, A. Milenin, Steel Res. Int. **81** (3), 224-233 (2010), DOI: 10.1002/srin.200900132.

[2] M. Kawulokova, B. Smetana, S. Zla, A. Kalup, E. Mazancova, P. Váňova, P. Kawulok, J. Dobrovska, S. Rosypalova, J. Therm. Anal. Calorim. **127** (1), 423-429 (2017), DOI: 10.1007/s10973-016-5780-4.

[3] R. Kawulok, I. Schindler, P. Kawulok, S. Rusz, P. Opěla, Z. Solowski, K.M. Čmiel, Metalurgija. **54** (3), 473-476 (2015).

[4] R. Kawulok, I. Schindler, P. Kawulok, S. Rusz, P. Opěla, J. Kliber, Z. Solowski, K.M. Čmiel, P. Podolinsky, M. Mališ, Z. Vašek, F. Vančura, Metalurgija **55** (3), 357-360 (2016).

[5] A. Grajcar, M. Opiela, J. Achiev. Mater. Manuf. Eng. **29** (1), 71-78 (2008).

[6] D. Jandová, L. Vadovicová, in: Metal 2004, Ostrava: Tanger Ltd, paper no. 223 (2004).

[7] https://www.indiamart.com/proddetail/heat-treatment-63227 30912.html

[8] H.J. Xie, X.C. Wu, Y.A. Min, J. Iron Steel Res. Int. **15** (6), 56-61 (2008).

[9] J. Calvo, I.H. Jung, A.M. Elwazri, D. Bai, S. Yue, J. Mater. Sci. Eng. A. **520** (1-2), 90-96 (2009).

[10] S.K. Liu, L. Yang, D.G. Zhu, J. Zhang, Metall. Mater. Trans. A, **25** (9), 1991-2000 (1994).

[11] D.J. Mun, E.J. Shin, Y.W. Choi, S.J. Lee, Y.M. Koo, J. Mater. Sci. Eng. A. **545**, 214-224 (2012).

[12] E. Rożniata, R. Dziurka. Arch. Metall. Mater. **60** (1), 497-502 (2015).

[13] H. Kawata, K. Fujiwara, M. Takahashi. ISIJ Int. **57** (10), 1866-1873 (2017).

[14] V.M. Khlestov, E.V. Konopleva, H.J. McQueen, Mater. Sci. Technol. **18** (1), 54-60 (2002).

[15] R. Kawulok, I. Schindler, J. Mizera, P. Kawulok, S. Rusz, P. Opěla, P. Podolinsky, K.M. Čmiel, M. Mališ, Arch. Metall. Mater. **63** (1), 55-60 (2018).

[16] A. Timoschenkov, P. Warczok, M. Albu, J. Klarner, E. Kozeschnik, G. Gruber, Ch. Sommitsch, Steel Res. Int. **85** (6), 954-967 (2014).

[17] L.X. Du, H.L. Yi, H. Ding, X.H. Liu, G.D. Wang, J. Iron Steel Res. **13** (2), 37-39 (2006).

[18] M. Aranda, B. Kim, R. Rementeria, C. Capdevila, C.G. Andrés, Metall. Mater. Trans. A. **45**, 1778-1786 (2014).

[19] T. Domański, W. Piekarska, M. Kubiak, Z. Saternus, Procedia Eng. **136**, 77-81 (2016). DOI: 10.1016/j.proeng.2016.01.177

[20] ČSN EN 10084-1998, Case hardening steels – Technical delivery conditions, Czech Standards Institute, 2000 Prague.

[21] I. Schindler, P. Kawulok, Hutnické listy. **66** (4), 85-90 (2013).

[22] P. Motyčka, M. Kövér, in: Comat 2012, Pilsen: Tanger Ltd, paper no. 1237 (2012).

[23] C. Qiu, S. Zwaag, Steel Res. Int. **68** (1), 32-38 (1997).

[24] P. Šimeček, R. Turoň, D. Hajduk, in: 68th Congress ABM 2013, Belo Horizonte, Brazil: Associação Brasileira de Metalurgia, paper no. 34 (2013).

[25] Z. Liu, K.F. Yao, Z. Liu, Mater. Sci. Technol. **16**, 643-647 (2000).

[26] Y. Xu, G. Xu, X. Mao, G. Zhao, S. Bao, Metals. **7** (9), 330 (2017), DOI: 10.3390/met7090330.